Gold atomic cluster mediated electrochemical aptasensor for the detection of Lipopolysaccharide

Biyas Posha, Sindhu R Nambiar, N. Sandhyarani

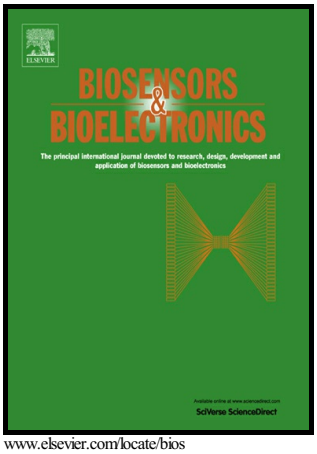

www.elsevier.com/locate/bios

PII: S0956-5663(17)30698-X
DOI: https://doi.org/10.1016/j.bios.2017.10.030
Reference: BIOS10055

To appear in: *Biosensors and Bioelectronic*

Received date: 1 August 2017
Revised date: 28 September 2017
Accepted date: 14 October 2017

Cite this article as: Biyas Posha, Sindhu R Nambiar and N. Sandhyarani, Gold atomic cluster mediated electrochemical aptasensor for the detection of Lipopolysaccharide, *Biosensors and Bioelectronic,* https://doi.org/10.1016/j.bios.2017.10.030

Gold atomic cluster mediated electrochemical aptasensor for the detection of Lipopolysaccharide

Biyas Posha[1], Sindhu R Nambiar[1,2], N. Sandhyarani[1*]

[1]Nanoscience Research Laboratory, School of Nano Science and Technology, National Institute of Technology, Calicut-673601

[2]Presently at CSIR-Central Electrochemical Research Institute, Karaikudi-630006,
*Corresponding author , sandhya@nitc.ac.in, phone:+91 495 2286537

Abstract

We have constructed an aptamer immobilized gold atomic cluster mediated, ultrasensitive electrochemical biosensor (Apt/AuAC/Au) for LPS detection without any additional signal amplification strategy. The aptamer self-assemble onto the gold atomic clusters makes Apt/AuAC/Au an excellent platform for the LPS detection. Differential pulse voltammetry and EIS were used for the quantitative LPS detection. The Apt/AuAC/Au sensor offers an ultrasensitive and selective detection of LPS down to 7.94×10^{-21} M level with a wide dynamic range from 0.01 attomolar to 1picomolar. The sensor exhibited excellent selectivity and stability. The real sample analysis was performed by spiking the diluted insulin sample with various concentration of LPS and obtained recovery within 2% error value. The sensor is found to be more sensitive than most of the literature reports. The simple and easy way of construction of this sensor provides an efficient and promising detection of an even trace amount of LPS.

Key words: Endotoxin, Lipopolysaccharide, Septic shock, Au atomic cluster, Aptasensor

1. Introduction

Endotoxins, also known as lipopolysaccharides (LPS), are the major component of the outer membrane of gram-negative bacteria, which is greatly contributing to maintain cell wall integrity. The higher amount of LPS released from the dead bacteria cells and a small amount of LPS released during their normal metabolism produces toxic effects on human (C. Venet 2000; Cohen 2000). LPS can be divided into three different regions: core polysaccharide, O-specific antigen and a unique structure of lipid moiety called lipid A, which is the main reason for the toxicity. Even minimal amount of endotoxin can cause fever, pyrogenicity, septic shock and may also lead to vascular blood clotting and multi-organ failure (Danner et al. 1991). LPS is a significant contaminant in pharmaceutical products and industrial food products. Food and drug administration (FDA) has set 0.2 endotoxin unit (EU, 1 EU ≈100pM) per kg body weight as the maximum acceptable level for drug distribution in the United States. Hence the detection and removal of LPS are of great concern in therapeutics, blood purification, and food industry. The Limulus amebocyte lysate (LAL) assay is the currently employed technique for the quantitative detection of bacterial endotoxin. The LAL assay consists of a coagulation reaction of hemotocytes lysate extracted from horseshoe crabs while exposing to LPS (Iwanaga 2007). Conventional LAL assay based on the photometrical detection is sensitive. However, its low reproducibility, the requirement of dedicated technicians, elaborated experiment setup, incapability to produce rapid response are the major drawbacks.

Other methods developed for LPS sensing includes optical sensors (Hawk and Armani 2015; Xu et al. 2017), fluorescence based sensors (Lv et al. 2015), photoelectrochemical immunosensors (Yang et al. 2015), sensors based on a quartz crystal microbalance (Chauhan et al. 2015), SPR based sensors (Patching 2014), etc. However, these methods still require tedious sample preparation procedures and dedicated technicians for reliable data. At this context, sensing based on electrochemical methods has come in the limelight owing to their simplicity, low cost, and ease of handling (Clement et al. 2001). Compared to other techniques electrochemical systems have advantages such as fast response, reproducibility, stability, the capability of multiplexed analysis, miniaturization and high sensitivity.

Different electrochemical techniques have been developed for LPS detection using bio-receptor molecules such as aptamers, peptides, and enzymes which show high affinity towards LPS (Ding et al. 2007; Kato et al. 2007; Su et al. 2012; Ansari et al. 2017). Among

different receptors aptamers are artificial nucleic acid ligands with high specificity and affinity for their targets and have wide applicability and long-term storage (Ellington and Szostak 1990; Famulok et al. 2000; Willner and Zayats 2007). They are made up of single-stranded DNA oligonucleotides or RNA, and owing to their desirable properties, they have been used as appropriate probes for the construction of various aptasensors (Bai et al. 2012; Bai et al. 2011; He et al. 2012; Zhu et al. 2011). While recognizing the target during the binding event, aptamers undergo significant structural rearrangement, and that can be exploited into a facile signal.

Su *et al.* fabricated an electrochemical impedance label-free aptasensor by aptamer immobilized gold electrode by employing a linker, 3-mercaptopropionic acid for LPS detection (Su et al. 2012). This impedance based aptasensor is capable of detecting LPS at a concentration range from 1pg ml^{-1} to 1ng ml^{-1}, the lower sensitivity restricts its wide application. Later, Bai *et al.* constructed an aptasensor based on electrochemical technique for LPS detection by adopting enzymatic recycling strategy to develop a three-way DNA junction (Bai et al. 2014). They have employed a nanohybrid of graphene and toluidine blue decorated with gold nanoparticle for signal amplification, and its LOD is found to be 8.7 fg ml^{-1}. This sensor achieved an excellent sensitivity however, the fabrication of the aptasensor is a tedious process. Mayall *et al.* (Mayall et al. 2017) recently developed an impedance sensor by immobilizing human toll-like receptor on a micro gold electrode *via* 11-mercaptoundecanoic acid as self-assembled monolayer for the detection of LPS however, the detection limit is only 1 ng ml^{-1}.

The introduction of gold atomic clusters (AuAC) to electrochemical biosensors has attracted much attention owing to their shape-/size-dependent physical and chemical properties. Atomic quantum clusters, between 2 and 150 atoms are stable clusters and are considered as a missing link between single atom and plasmonic nanoparticles, with average particle size in the range of 0.5–2 nm. AuAC possesses properties such as fast electron transfer, good water solubility, excellent biocompatibility, high surface area, stability and facile synthesis (Li et al. 2011). They exhibit unique properties through quantum size effects and have high surface to volume ratio resulting in a large number of binding sites available for catalysis or chemical sensing (Chen and Goodman 2004; Jeyabharathi et al. 2010a; Nambiar et al. 2013).

In the present work, we report for the first time a highly sensitive gold cluster mediated electrochemical aptasensor for the detection of LPS without any additional signal

amplification strategy. The amino terminated aptamer was immobilized on the electrochemically synthesized AuAC on the Au electrode surface, through the strong affinity of 5' end amino groups of the aptamer (Apt) with Au atomic cluster. The amine-gold surface can form charge-neutral interaction by weak covalent bond, they can also prevent agglomeration of clusters due to particle stability, which is kinetic rather than thermodynamic in nature (Leff et al., 1996). The covalent binding between 5' end amino groups and Au clusters produces a highly stable Apt/AuAC/Au electrode for LPS detection. We have utilised the allowed or blocked electron transfer through the assembled molecules on the surface to monitor the concentration of target molecule. On taking account of the steric hindrance offered by the LPS molecule, a very high sensitivity could be demonstrated. The process of sensor fabrication is very simple when compared with other electrochemical sensors for LPS. The developed sensor provided a higher sensitivity than literature reports, and the limit of detection is in attomolar level with a linear response of 9 orders of magnitude.

2. **Materials and Experimental Methods**

2.1 Materials

Endotoxin standard was purchased from Sigma-Aldrich. The HPLC-purified DNA oligonucleotide (aptamer) 5'–NH_2–$(CH_2)_6$-CTTCTGCCCGCCTCCTTCCTAGCCGGATCGCGCTGGCCAGATGATATAAAGGGTC AGCCCCCCAGGAGACGAGATAGGCGGACACT-3' was purchased from Integrated DNA Technologies, USA and stored at -20°C before use. Cetyltrimethyl ammonium bromide (CTAB) was purchased from SRL chemicals. Glucose and bovine serum albumin (BSA) were purchased from Merck, India. Ascorbic acid was purchased from Himedia. Dopamine was purchased from Sigma-Aldrich. $K_3[Fe(CN)_6]$ and KCl were purchased from Merck. All solutions were prepared with deionised distilled water with a resistivity of 18.2MΩcm through a Millipore MilliQ water purification system. Phosphate buffered solutions (PBS, 0.1 M, pH 7.4) containing 0.1 M KH_2PO_4, and 0.1M NaOH were used throughout the experiment. All other chemicals were of reagent grade and used as received.

2.2 Instrumentation

Electrochemical experiments were performed at room temperature using CHI 760E electrochemical workstation (CH Instruments, Texas, Austin). A standard three-electrode system was employed with Pt wire as counter electrode, Ag/AgCl as reference electrode and electrochemically cleaned gold disk electrode (CH Instruments Texas, Austin; diameter: 2mm) with a sensitive area of 0.0314 cm^2 was used as the working electrode. DPV measurements were performed in 0.1 M PBS (pH 7.4). All the details used for electrochemical measurements are indicated in respective sections. EIS data was fitted by a ZSimpWin software with an appropriate equivalent circuit. The size and morphology were studied using high-resolution transmission electron microscopy (HR-TEM) on FEI Technai G2 T20 instrument with an accelerating voltage of 200 kV. The UV-visible (UV-vis) spectroscopy was performed on a UV-1800 Shimadzu spectrometer in the range of 200–800 nm with quartz cuvette of path length 1 cm. XPS measurements were carried out on a Kratos Nova Photoelectron Spectrometer with a monochromatic Al Kα source (1486.6 eV) operating at 150W.

2.3 Fabrication of Au atomic cluster –Aptamer (Apt/AuAC/Au) modified electrode.

Before modification, gold disk electrode was polished with alumina slurry (0.3µm and 0.05µm) and washed thoroughly with water. The freshly polished electrode was then sonicated in ethanol followed by DI water for a couple of times. Further, cleaning was carried out by potential cycling between 0.2 V and 1.5 V in 0.1 M $HClO_4$ at a scan rate of 100 mV S^{-1} for 22 cycles. This is followed by sonication of electrode for 2 minutes in DI water and dried before modification. Au atomic cluster (AuAC) modified gold electrode was prepared by cycling in the potential range from 0 V to 1.2 V for 20 times in aqueous CTAB solution (50 mM) at a scan rate of 100mV/s (Jeyabharathi et al. 2010b). The cyclic voltammogram of the deposition is given in Figure S1. The AuAC modified Au electrode was rinsed with water and dried in air. The concentration and incubation time for aptamer to obtain the complete coverage of the AuAC/Au surface was optimised (Figure S.2 and S.3). 2 µM concentration of aptamer with an incubation time of 3 hours is found to be adequate to produce a complete surface coverage on AuAC/Au electrode. 6 µL of 2 µM aptamer was immobilized on AuAc/Au electrode by drop casting and kept for drying at 25°C for 3 hours. The electrode was again washed with DI water to remove the unbounded aptamer and the Apt/AuAC/Au electrode dried in air. Further, the electrode Apt/AuAC/Au was immersed in 1 mM BSA for 1

minute, in order to avoid the nonspecific binding of analyte, and again rinsed with DI water and dried in air. The Apt/AuAC/Au electrode was used for the detection of endotoxin. A schematic diagram depicting the fabrication and working of Apt/AuAC/Au sensor is shown in Scheme 1.

2.4 Detection/quantification procedure

Different concentrations of LPS stock solutions were prepared from 100aM to 1nM. 10µL from each LPS stock solutions were added to 10mL of 0.1M PBS solution during quantitative electrochemical measurements. Differential pulse voltammetry (DPV) was monitored for the LPS detection by scanning the potential from 0.6 to 0V at an amplitude and frequency of 50 mV and 10 Hz respectively. The LPS quantification was achieved by monitoring the reduction peak current produced by AuAC at 0.34V.

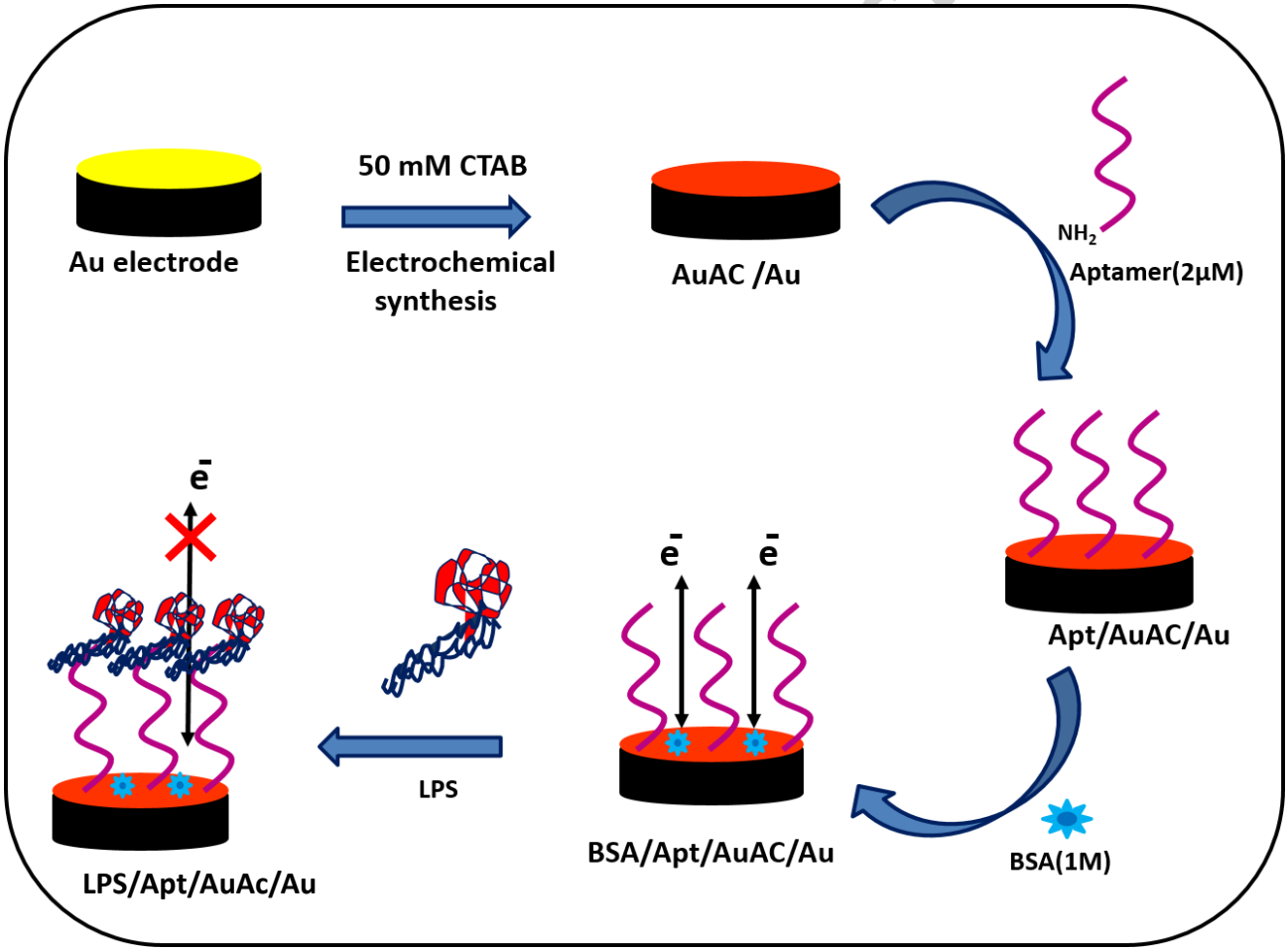

Scheme 1: Schematic representation of the fabrication and working principle of

Apt/AuAC /Au sensor.

3. Results and discussion

3.1 Morphological and spectroscopic studies of AuAC

The electrochemically synthesized AuAC was characterized by HR-TEM, X-ray photoelectron spectroscopy, UV-visible spectroscopy and dynamic light scattering studies. For HR-TEM samples were prepared by dispersing Au atomic cluster in 1mM aqueous CTAB and immediately drop casting on carbon-coated copper grid. Fig.1.A exhibits the TEM image of AuAC, which shows the AuAC with particle size ranging from 1nm to 5nm. The structural instability of AuAC can be attributed to their tendency to aggregate when they are exposed to intense electron beam (Iijima and Ichihashi 1986). Moreover, the poor contrast exhibited by the TEM images can be account to the presence of subnanometer sized entities. (Menard et al. 2006). Dynamic light scattering (DLS) studies were carried out to understand the size distribution of Au atomic clusters. AuAC formed on the electrode surface was immediately collected in water containing 50mM CTAB in order to avoid agglomeration. DLS curve shows the particle size distribution ranging from 0.5 to 2nm. The DLS did not show any peak above 10nm confirming that all the clusters formed are below 10nm size.

Fig.1.B shows the UV-visible spectrum of AuAC with a peak maximum at 393 nm and minor peak at 475 nm. Above peaks are attributed to the electronic transitions of interband sp←d and intraband sp←sp respectively. The higher intensity of the peak at 393nm suggests the molecular like behaviour of the cluster formed with a size of approximately 2 nm as reported elsewhere (Jeyabharathi et al. 2010a; Zhang 1997). Moreover, the absorbance spectrum shows the complete absence of the SPR band which rule out the presence of Au nanoparticle. Further, this evidence the formation of the Au in the form of individual clusters and its stability. The peak at 270 nm correspond to the CTAB present in the solution.

X-ray photoelectron spectroscopy (XPS) measurements were carried out on the AuAC on Au electrode to get an insight in the oxidation state of Au clusters. Fig.1.C shows the XPS spectrum of Au4f region. Au4f signal is deconvoluted into four individual peaks. Peaks I and II are attributed to Au $4f_{7/2}$ (84.17 eV) and Au $4f_{5/2}$ (87.87 eV) lines of Au (0) with a binding

energy (B. E) difference of 2.16 V. While, the peaks III and IV can be assigned to Au $4f_{7/2}$ (86.33 eV) and Au$4f_{5/2}$ (90.01 eV) of Au (I) respectively. The slightly low intense peaks I and II are mainly from the Au (0) of the AuAC however, the minor contribution from the bulk Au substrate cannot be neglected. Further there is no peak at higher B. E, which indicates the absence of Au (III) in AuAC. In addition to this, larger area of Au (I) in comparison to Au (0) clearly reveals that the major component in clusters is Au (I). In short, XPS data gives a solid support for the AuAC oxidation states that obtained during the redox process of Au (0)-Au (I) in the electrochemical synthesis of AuAC. The electrochemical mechanism of AuAC formation can be explained as follows. During the anodic scan Au (0) is oxidized to Au (I) and deposited on the electrode surface. During the cathodic scan some of this Au (I) accept one electron and reduced back to Au (0) which is also deposited on the electrode surface. Thus after completing 20 potential cycles in CTAB numerous clusters composed of Au (I) and Au (0) are formed on the gold electrode surface. CTAB acts as a supporting electrolyte during the redox process in addition to stabilizing the Au clusters formed on the electrode surface. An orange red film can be observed on the electrode surface which indicates the electrogenerated thin layer of AuAC.

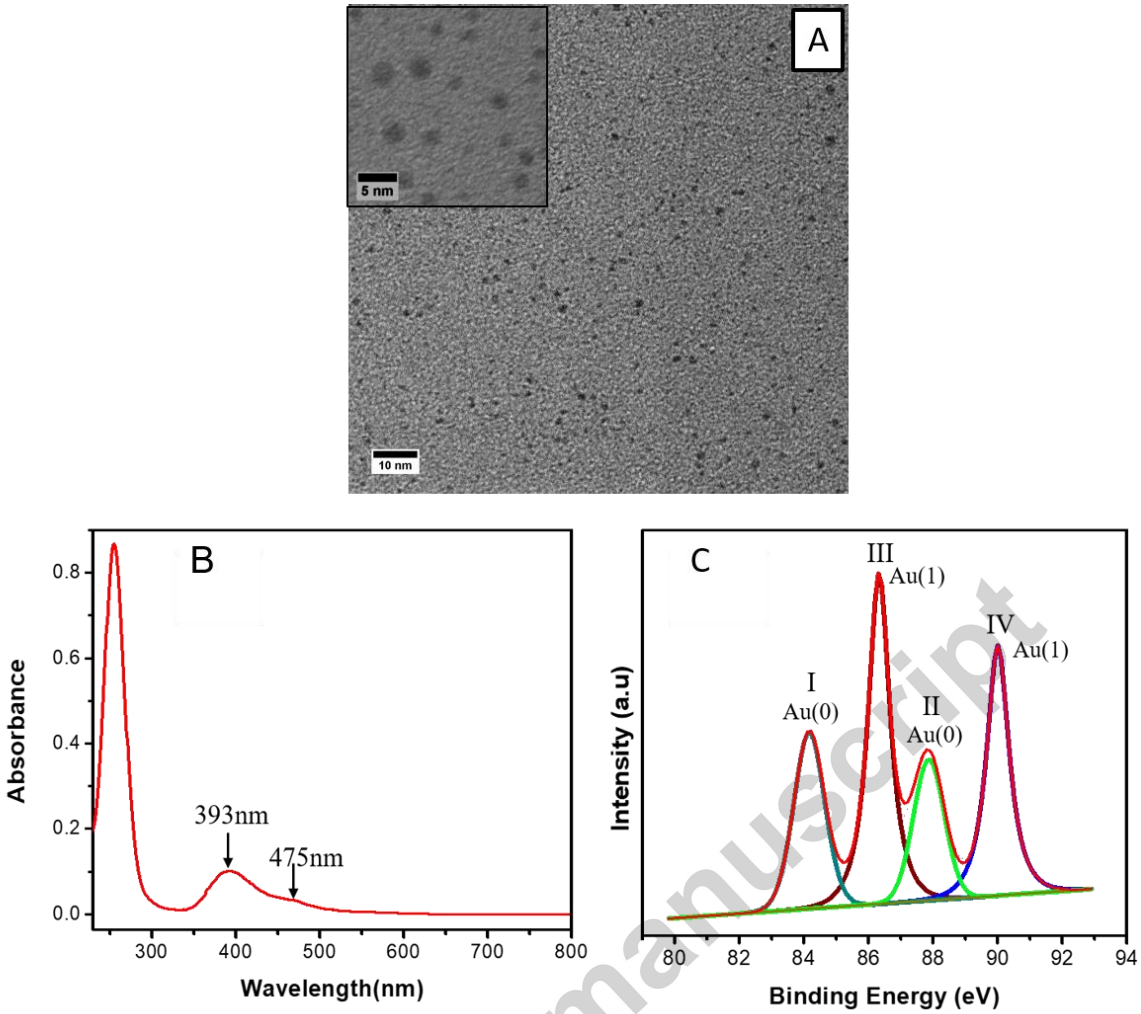

Fig.1(A) HR-TEM image of AuAC (inset-magnified image) (B) UV-Visible absorption spectrum of AuAC (C) X-ray photoelectron spectrum of AuAC in the Au 4f region

3.2 Electrochemical behaviour AuAC/Au and Apt/AuAC/Au modified electrode

To understand the electrochemical properties of AuAC/Au and Apt/AuAC/Au modified electrode, cyclic voltammetry (CV) were carried out with $K_3[Fe(CN)_6]$ as a probe. Figure S.4 shows the CV profile of (a) bare Au (b) AuAC/Au (c) Apt/AuAC/Au in 5 mM $K_3[Fe(CN)_6]$ with 0.1 M KCl as supporting electrolyte in the potential range 0V to 0.6V Vs Ag/AgCl at a scan rate of 100 mV/s. In the case of bare gold electrode, the peak potential difference (ΔEp) of 143mV (Ipc/Ipa $\approx$ 1; curve a) was observed, which indicates a quasi-reversible redox reaction. Whereas in the case of AuAC/Au electrode, the anodic peak current decreased considerably while ΔEp is 178mV (curve b), which indicates the slow redox reaction of $K_3[Fe(CN)_6]$ at the interface due to the thin layer of insulating AuAC formed at the Au

substrate. After the immobilization with aptamer, a small shift in the redox peaks toward positive potential is obtained with a slight increment in the redox current, indicating the proper binding of aptamer on AuAC modified electrode with a ΔEp of 135mV (curve c). The changes in the current response during each stage of modification of Au electrode reveals the formation of AuAC thin film and the proper immobilization of aptamer.

Electrochemical impedance spectroscopy (EIS) studies were employed to monitor the charge transfer process existing at the electrode interface during electrode fabrication process. Fig.2.A illustrate the Nyquist plot from the EIS of different modified electrodes in the presence of 5 mM K_3 [$Fe(CN)_6$] containing 0.1 M KCl. EIS data was fitted with a modified Randles circuit, which is shown in figure. All the curves have similar features a small semicircle domain at high frequencies and an almost straight line at low frequencies indicates diffusion. The (curve a) represents bare gold (Au), which had a relatively low resistance with a small semicircle domain and the Rct is found to be 115Ω. After the deposition of gold atomic cluster on the polycrystalline gold (AuAC/Au) the diameter of semicircle increased with Rct of 174Ω (curve b) indicates a slow charge transfer process. This is attributed to the insulating nature of gold atomic clusters having Au (I) and the adsorbed CTAB at the electrode interface, which reduces the electron transfer. After the assembly of aptamer onto the electrode surface (Apt/AuAC/Au) the semicircle domain decreased with a Rct of 141Ω (curve c). The decrease in charge transfer resistance at the electrode interface is attributed to the proper binding of aptamer with AuAC through the 5’ end amino groups present in the aptamer with the replacement of some of the bulky CTAB adsorbed during cluster formation, which in turn enhance the electron transfer and thus electrochemical activity of the final modified electrode Apt/AuAC/Au. The EIS results confirms the successful immobilization of aptamer on AuAC/Au electrode.

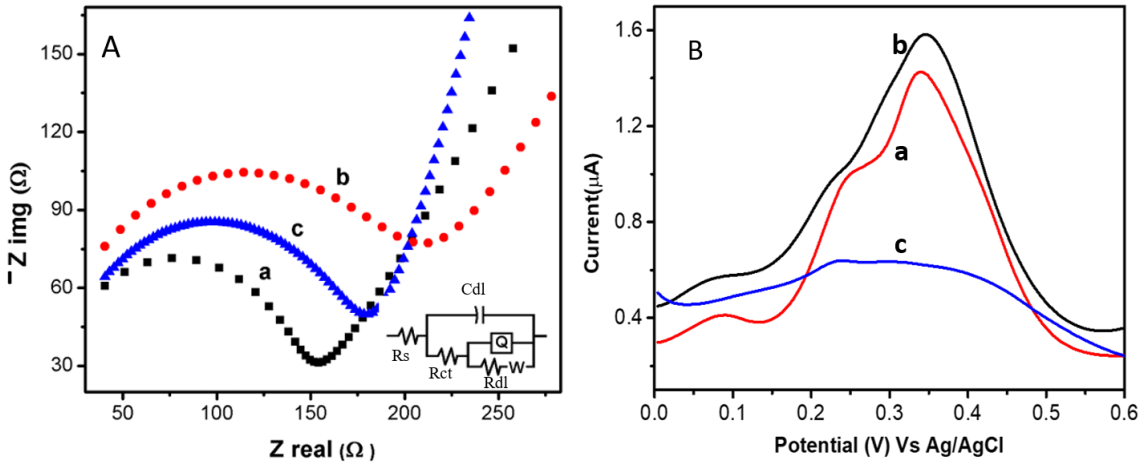

Fig.2. (A) EIS response obtained at (a)bare Au, (b) AuAc/Au and (c) Apt/AuAC/Au in 5mM $K_3Fe(CN)_6$ and 0.1 M KCl as a supporting electrolyte. (B) DPV response of (a) AuAC/Au, (b) Apt/AuAC/Au and (c) 1pM LPS@ Apt/AuAC/Au in 0.1M PBS.

The electrochemical properties of the modified Apt/AuAC/Au and AuAC/Au electrodes were further studied by differential pulse voltammetry (DPV). Fig.2.B shows the DPV response of AuAC/Au, Apt/AuAC/Au, and 1pM LPS@Apt/AuAC/Au in 0.1M PBS solution. AuAC/Au electrode shows a peak current of 1.426 µA at 0.340V, which is attributed to the reduction of Au(I) to Au(0) at the electrode surface (curve a). After the immobilization of aptamer on AuAC/Au electrode, the peak current increased to 1.582 µA, indicating more reduction of clusters at the electrode surface (curve b). This enhancement in the reduction peak current can be attributed to the replacement of some of the sterically hindered CTAB with less sterically hindered aptamer, which increases the electron transfer at the electrode-solution interface. When the Apt/AuAC/Au electrode was incubated in 1pM LPS, the current response drastically reduced from 1.582µA to 0.6192µA (curve c). This confirms the selective binding of LPS at the Apt/AuAC/Au electrode owing to the strong affinity of LPS towards aptamer. The strongly adsorbed LPS acts as an insulating layer at the electrode surface and block the electron transfer between the solution and electrode. Therefore, the reduction peak current of Apt/AuAC/Au electrode can be used as an efficient probe for LPS detection, by monitoring the peak current at varying concentration of LPS.

3.3 Analytical performance characteristics

The performance of this sensor for the detection of LPS at different concentrations and its repeatability were evaluated. Fig.3.A depicts the differential pulse voltammetric responses of the proposed sensor obtained for the different concentrations of LPS under physiological conditions of pH 7.4 in 0.1M PBS. The peak current obtained for Apt/AuAC/Au electrode at 0.344V, which is attributed to the reduction of Au (I) to Au (0) at the electrode surface. This peak current due to reduction of clusters can be used as a probe for sensing the target molecules (Aneesh et al., 2014). From the DPV curves, it can be seen that the peak current of Apt/AuAC/Au electrode (1.582µA, the blank signal, ie., without LPS in 0.1M PBS alone) decreases upon increasing the concentration of LPS. The decrease in peak current of Apt/AuAC/Au electrode can be attributed to the insulating nature of the interface formed by the target LPS upon the specific binding with the self-assembled aptamer on the AuAC/Au. The steric hindrance of the LPS at the electrode interface prevents the electron transfer to the electrode surface and act as a barrier for the reduction of Au (I) to Au (0) leading to the decrease in reduction peak current.

Fig.3.B illustrates the calibration plot of quantitative detection of the target LPS, ΔIp (difference in current produced by the Apt/AuAc/Au electrode and the current produced upon the addition of LPS concentrations) *versus* logarithm of LPS concentration. The ΔIp was shown a linear response to the logarithm of the target LPS from 0.01 atto molar to 1pico molar with a correlation coefficient of 0.9959. The developed electrode could be applied for a wide range of concentrations. The limit of detection (LOD) was calculated to be 7.94×10^{-21} M at 3σ based on standard deviation of the blank signal (n=3). The relative standard deviation (RSD) was found to be 4.66% for 5 successive determinations of (0.01aM) LPS which shows the extremely high precision of the designed LPS sensor.

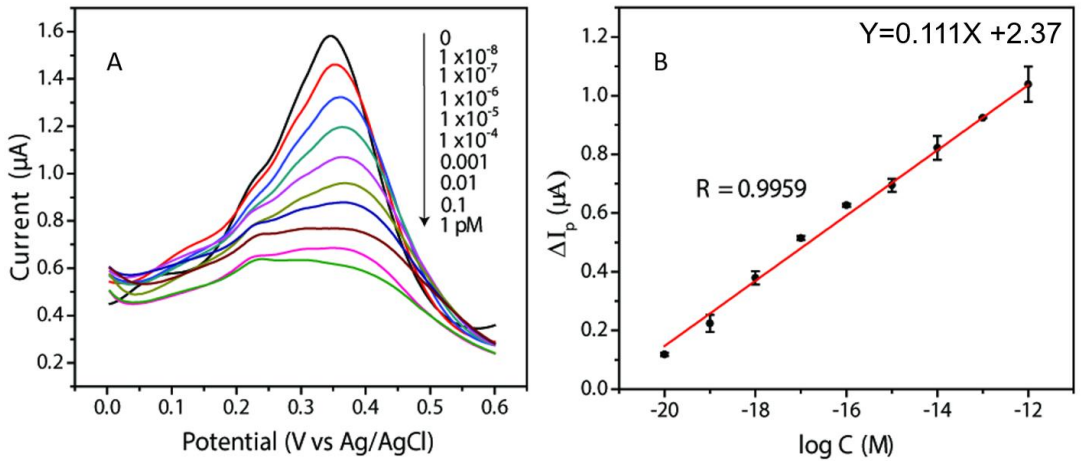

Fig.3. (A) DPV responses of the Apt/AuAc/Au sensor incubated with different concentration of LPS in 0.1 M PBS. (B) Calibration plot of ΔIp versus the logarithm value of LPS concentration.

The recognition event of LPS with aptamer immobilized AuAC/Au electrode surface was further studied by impedance spectroscopy in the presence of 5mM $K_3[Fe(CN)_6]$ redox couple in 0.2 M PBS buffer. All the EIS were carried out in a frequency range of 0.1 to 10^6 Hz at amplitude of 0.005 V and the potential applied was the onset potential 0.24V. Fig.4.A shows the Nyquist plots of Apt/AuAC/Au in a wide dynamic range of LPS concentration. EIS data were fitted to an appropriate equivalent circuit (shown in Fig.4.A). Rs, x-intercept at the high frequency region, represent the solution resistance (≈123Ω) and intact in different concentration of LPS. This is followed by a near semicircle, which is represented by the rest of the element in the circuit. The semicircle is mainly decided by a Q1, an imperfect capacitance and a charge transfer resistance (Rct). Rct is mainly attributed to the interfacial resistance at the electrode interface for the electron transfer from the solution based $Fe(CN)_6^{3-/4-}$ to the electrode. Other minor components contributing are Q2, Rdl and Wd, corresponds to a pseudo capacitance, double layer resistance, and diffusion resistance respectively. After fitting all the EIS spectra at LPS concentration ranging from 0.01 attomolar to 1 picomolar, it is found that the Rct is solely sensitive to the LPS concentration. Fig.4.B exhibits the calibration plot of Rct with the logarithmic concentration of LPS with a linear regression coefficient, R= 0.9830 concentration ranging from 0.01aM to 1 pM. From the Fig.4.B, it can be seen that the charge transfer resistance (Rct) increases with the successive addition of

LPS. The enhancement in the Rct value can be attributed to the fact that the specific binding of LPS with aptamer resulting a steric hindrance at the interface blocking electron-transfer, which would slowdown the oxidation/reduction of the $[Fe(CN)_6]^{4-/3-}$ redox probe. In addition to the DPV results, the linear response of Rct with the logarithmic concentration of LPS confirms, that Apt/AuAC/Au sensor is capable of an effective detection of LPS down to attomolar level.

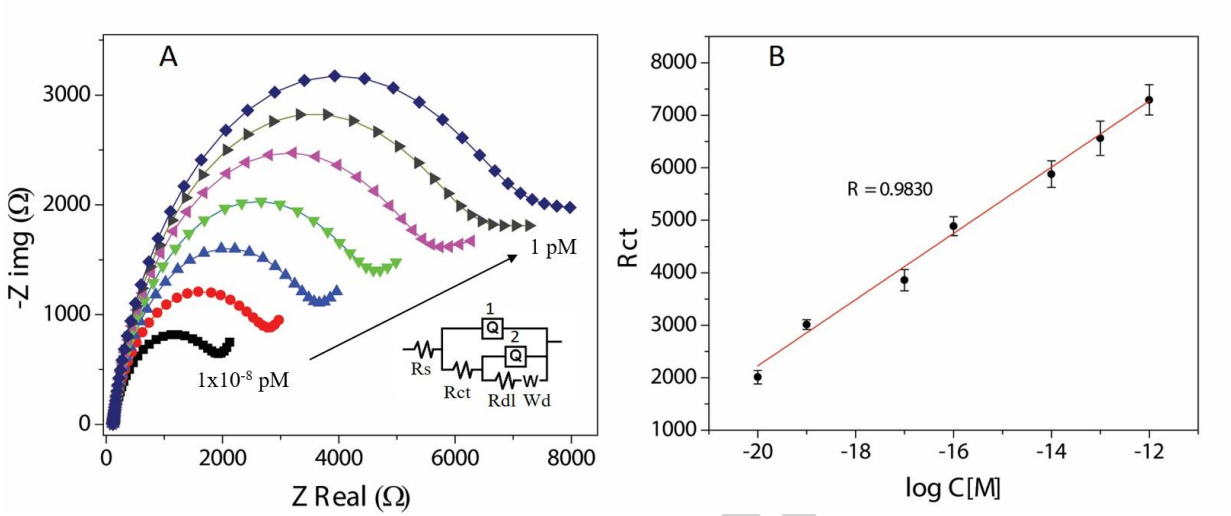

Fig.4.A The EIS response of Apt/AuAc/Au sensor incubated with different concentration of LPS from $1x10^{-8}$ pM to 1 pM in 5mM $K_3[Fe(CN)_6]$ and 0.2M PBS as an electrolyte. Fig.4.B calibration plot of Rct versus logarithm of LPS concentration. All measurements were done in triplicates.

3.4 Selectivity and stability of the Apt/AuAC/Au sensor

DPV experiments were carried out to check the cross-reactivity of the LPS with possible coexisting and interfering compounds, such as Ascorbic Acid (AA), Bovine serum Albumin (BSA), glucose, and Dopamine (DA). The Apt/AuAC/Au electrode was incubated in different concentrations of interfering compounds from 100 attomolar to 1µM in 0.1M PBS (pH 7.4). For a wide range of concentration of interfering compounds, from 100 attomolar to 1µM, the ΔIp produced by the Apt/AuAC/Au sensor is almost similar. The successive addition of higher concentrations of interfering compounds did not make any appreciable increment in ΔIp, unlike in the case of LPS, shows that the proposed sensor exhibits remarkable selectivity towards LPS. This can be attributed to the high specificity of the

Apt/AuAC/Au sensor to LPS. Fig.5 shows the selectivity data of 1 pM LPS versus 100 times higher concentration of interfering compounds (100 pM). The difference in ΔIp, indicates that the developed sensor showed a negligible cross-reactivity towards AA, BSA, glucose, and DA.

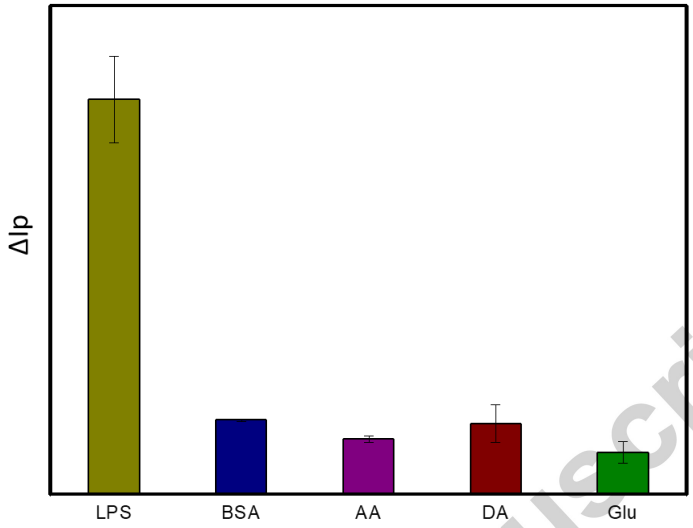

Fig.5 Selectivity of the Apt/AuAc/Au sensor; detection of LPS 1pM against the interference compounds: AA (100 pM), DA (100 pM), glucose (100 pM), BSA (100 pM).

The stability of the Apt/AuAC/Au electrode was also studied by storing the electrode at 4ºC for 1 week. It was found that 95.54% of the signal was retained, which indicates that the sensor can offer excellent stability.

Real sample analysis were also conducted with clinical-grade insulin drug. DPV was used for the detection procedure. 50 µL of insulin was diluted in 10ml of PBS solution and spiked with a known amount of LPS. The linearlity is obtained from 1aM to 1pM (R= 0.9918) due to the matrix effect produced by the drug. The construced Apt/AuAC/Au electrode showed excellent recovery for various LPS concentrations as 100 fM (99.22%), 10 fM (99.14%), 100 aM (97.75%), 10 aM (100.352%) and 1aM (99.23%) indicating the use of the sensor we developed in the real sample analysis .

The performance of various electrochemical sensors used for LPS detection is summarised in Table S2. In comparison with the hitherto reported methods, the detection limit offered by the current method, is the lowest one. Moreover, the ultra-sensitive Apt/AuAC/Au electrode can

perform with wide calibration range along with high precision, when comparing with any of the previously reported electrochemical LPS sensors.

4. Conclusion

In summary, we have demonstrated a simple and novel electrochemical platform for the selective and sensitive detection of LPS based on an aptamer immobilized, Au atomic cluster mediated, electrochemical biosensor. This sensor is capable of detecting target LPS down to attomolar level. The electrochemical Apt/AuAC/Au sensor offers an attractive LOD of 7.94×10^{-21} M for LPS with a wide calibration range from 0.01aM to 1 pM. The sensor can be used for the detection of even trace amount of LPS in drugs/food/blood samples which is demonstrated with the real sample analysis of LPS concentration in the drug insulin. LPS spiked insulin gave the recovery within 2% error. The sensor exhibited very high selectivity and stability. Using this method it will be possible to fabricate a sensor for the real time measurement at patients bed side.

Acknowledgements

The authors gratefully acknowledge Kerala State Council for Science, Environment, and Technology (KSCSTE) for their financial support to the Nanoscience Research Laboratory. Department of Science and Technology (DST) and CSIR are acknowledged for the support for the biosensor research at nanoscience research laboratory. Acknowledgments are due to the funding for doctoral program (BP) and postdoctoral program (SRN) of higher education provided by the University Grant Commission.

References

Aneesh, P.K., Nambiar, S.R., Rao, T.P., Ajayaghosh, A., 2014. Phys. Chem. Chem. Phys. 16, 8529.

Ansari, N., Yazdian-Robati, R., Shahdordizadeh, M., Wang, Z., Ghazvini, K., 2017. Biochem. 533, 18–25.

Bai, L., Chai, Y., Pu, X., Yuan, R., 2014. Nanoscale 6(5), 2902-2908.

Bai, L., Yuan, R., Chai, Y., Yuan, Y., Wang, Y., Xie, S., 2012. Chemical Communications 48(89), 10972-10974.

Bai, L., Yuan, R., Chai, Y., Yuan, Y., Zhuo, Y., Mao, L., 2011. Biosensors and Bioelectronics 26(11), 4331-4336.

C. Venet, F.Z., A. Viallon, A. Ross, P. Pain, P. Gery, D. Page, R. Vermesch, M. Bertrand, F. Rancon, J. C. Bertrand, 2000. Intensive Care Medicine 26(5), 538-544.

Chauhan, R., Solanki, P.R., Singh, J., Mukherjee, I., Basu, T., Malhotra, B.D., 2015. Food Control 52, 60-70.

Chen, M., Goodman, D., 2004. Science 306(5694), 252-255.

Clement, R.E., Yang, P.W., Koester, C.J., 2001. Analytical chemistry 73(12), 2761-2790.

Cohen, J., 2000. Intensive Care Medicine 26(1), S051-S056.

Danner, R.L., Elin, R.J., Hosseini, J.M., Wesley, R.A., Reilly, J.M., Parillo, J.E., 1991. Chest 99(1), 169-175.

Ding, S.-J., Chang, B.-W., Wu, C.-C., Chen, C.-J., Chang, H.-C., 2007. Electrochemistry communications 9(5), 1206-1211.

Ellington, A.D., Szostak, J.W., 1990. Nature 346(6287), 818.

Famulok, M., Mayer, G., Blind, M., 2000. Accounts of Chemical research 33(9), 591-599.

Hawk, R.M., Armani, A.M., 2015. Biosensors and Bioelectronics 65, 198-203.

He, Y., Lin, Y., Tang, H., Pang, D., 2012. Nanoscale 4(6), 2054-2059.

Iijima, S., Ichihashi, T., 1986. Physical review letters 56(6), 616.

Iwanaga, S., 2007. Proceedings of the Japan Academy, Series B 83(4), 110-119.

Jeyabharathi, C., Senthil Kumar, S., Kiruthika, G.V.M., Phani, K.L.N., 2010a. A Angewandte Chemie International Edition 49(16), 2925-2928.

Jeyabharathi, C., Senthil Kumar, S., Kiruthika, G.V.M., Phani, K.L.N., 2010b. Angewandte Chemie International Edition 49(16), 2925-2928.

Kato, D., Iijima, S., Kurita, R., Sato, Y., Jia, J., Yabuki, S., Mizutani, F., Niwa, O., 2007. Biosensors and Bioelectronics 22(7), 1527-1531.

Leff, D. V., Brandt, L., Heath, J.R., 1996. Langmuir 12, 4723–4730.

Li, L., Liu, H., Shen, Y., Zhang, J., Zhu, J.-J., 2011. Analytical chemistry 83(3), 661-665.

Lv, Z., Liu, J., Bai, W., Yang, S., Chen, A., 2015. Biosensors and Bioelectronics 64, 530-534.

Mayall, R., Renaud-Young, M., Chan, N., Birss, V., 2017. Biosensors and Bioelectronics 87, 794-801.

Menard, L.D., Gao, S.-P., Xu, H., Twesten, R.D., Harper, A.S., Song, Y., Wang, G., Douglas, A.D., Yang, J.C., Frenkel, A.I., 2006. The Journal of Physical Chemistry B 110(26), 12874-12883.

Nambiar, S.R., Aneesh, P.K., Rao, T.P., 2013. Analyst 138(17), 5031-5038.

Patching, S.G., 2014. Biochimica et Biophysica Acta (BBA) - Biomembranes 1838(1, Part A), 43-55.

Su, W., Lin, M., Lee, H., Cho, M., Choe, W.S., Lee, Y., 2012. Biosens Bioelectron 32(1), 32-36.

Willner, I., Zayats, M., 2007. Angewandte Chemie International Edition 46(34), 6408-6418.

Xu, W., Tian, J., Shao, X., Zhu, L., Huang, K., Luo, Y., 2017. Biosens. Bioelectron. 89, 795–801.

Yang, J., Gao, P., Liu, Y., Li, R., Ma, H., Du, B., Wei, Q., 2015. Biosensors and Bioelectronics 64, 13-18.

Zhang, J.Z., 1997. Accounts of chemical research 30(10), 423-429.

Zhu, S., Han, S., Zhang, L., Parveen, S., Xu, G., 2011. Nanoscale 3(11), 4589-4592.

Aneesh, P.K., Nambiar, S.R., Rao, T.P., Ajayaghosh, A., 2014. Electrochemical synthesis of a gold atomic cluster–chitosan nanocomposite film modified gold electrode for ultra-trace determination of mercury. Phys. Chem. Chem. Phys. 16, 8529. doi:10.1039/c4cp00063c

Ansari, N., Yazdian-Robati, R., Shahdordizadeh, M., Wang, Z., Ghazvini, K., 2017. Aptasensors for quantitative detection of Salmonella Typhimurium. Anal. Biochem. 533, 18–25. doi:10.1016/j.ab.2017.06.008

Leff, D. V., Brandt, L., Heath, J.R., 1996. Synthesis and Characterization of Hydrophobic, Organically-Soluble Gold Nanocrystals Functionalized with Primary Amines. Langmuir 12, 4723–4730. doi:10.1021/la960445u

Xu, W., Tian, J., Shao, X., Zhu, L., Huang, K., Luo, Y., 2017. A rapid and visual aptasensor for Lipopolysaccharides detection based on the bulb-like triplex turn-on switch coupled with HCR-HRP nanostructures. Biosens. Bioelectron. 89, 795–801. doi:10.1016/j.bios.2016.10.012

Highlights

- A rapid and highly sensitive method for endotoxin quantification
- Reduction of gold atomic cluster is used to monitor the concentration of endotoxin
- Allowed or forbidden electron transfer through the assembled molecules are utilized for the detection
- Achieved a selective detection of LPS down to 7.94×10^{-21} M level.